Pilot Study Examining Spatial Differences in Water Quality Between Shoal and Channel Habitats

Taylor Winchell, Elizabeth Stumpner, Ariella Chelsky, and David Senn

1. Introduction

1.1 Motivation

Under the umbrella of the Nutrient Management Strategy (NMS; www.sfbaynutrients.sfei.org), we are investigating relationships between the SFB's elevated nutrient levels and phytoplankton production, with the goal of identifying protective nutrient loads and effective nutrient management options. To address these goals, NMS work includes continued ship-based monitoring (in collaboration with USGS); augmenting that monitoring with high-frequency sensor data and intensive field studies; and developing coupled hydrodynamic-biogeochemical models -- calibrated using field observations -- to simulate water quality under a range of forcings.

1.2 Background

San Francisco Bay (SFB) receives high loads of nitrogen (N) and phosphorus (P), but nonetheless experiences relatively low phytoplankton production compared to other nutrient-enriched estuaries. Observational data from sustained long-term monitoring and targeted investigations in SFB have played a critical role in informing our understanding of factors that control phytoplankton production (e.g., Cloern 1996) and tracking changes in production over time (Cloern et al., 2007; Cloern et al, 2010). The foundation of these observations come from four decades of biweekly to monthly ship-based sampling carried out by the USGS along SFB's deep channel "spine", complemented by intensive investigations of lateral variability.

The geomorphology of San Francisco Bay is defined by a deep channel surrounded by shallow shoals and intertidal mudflats. Studies during the 1980s and 1990s found that phytoplankton production and biomass can differ strongly between channel and shallow shoal environments, with those differences caused by lateral differences in physical (vertical mixing; light availability; lateral exchange) and biological (benthic or pelagic grazing) forcings (Cloern et al., 1985; Powell et al., 1989; Huzzey et al., 1990; Cloern, 1996; Thompson et al., 2008). Although shallow shoals are prominent features in multiple SFB subembayments (Suisun, San Pablo, South, Lower South), this report focuses on recent work conducted in South Bay, which has a shallow shoal (1-4m deep) region and intertidal mudflats (Figure 1) that comprise the majority of South Bay's area. The relatively large depth difference between these habitats is one of several factors that could contribute to differences in light availability, and therefore lateral differences in phytoplankton production and biomass (Figure 2).

We hypothesized that phytoplankton biomass (as measured by chl-a), gross primary production, and other related parameters would differ substantially between South Bay shoal and adjacent channel habitats. Furthermore, we hypothesize that accounting for these differences (including in the calibration of numerical models), is necessary for predicting phytoplankton production, nutrient utilization, and the nutrient:phytoplankton inter-relationships within SFB. To test these hypotheses, we conducted three pilot deployments of a mooring equipped with high-frequency biogeochemical sensors, and compared

shoal observations with high-frequency observations collected at nearby channel sites. This report describes initial observations from those deployments and identifies proposed next steps.
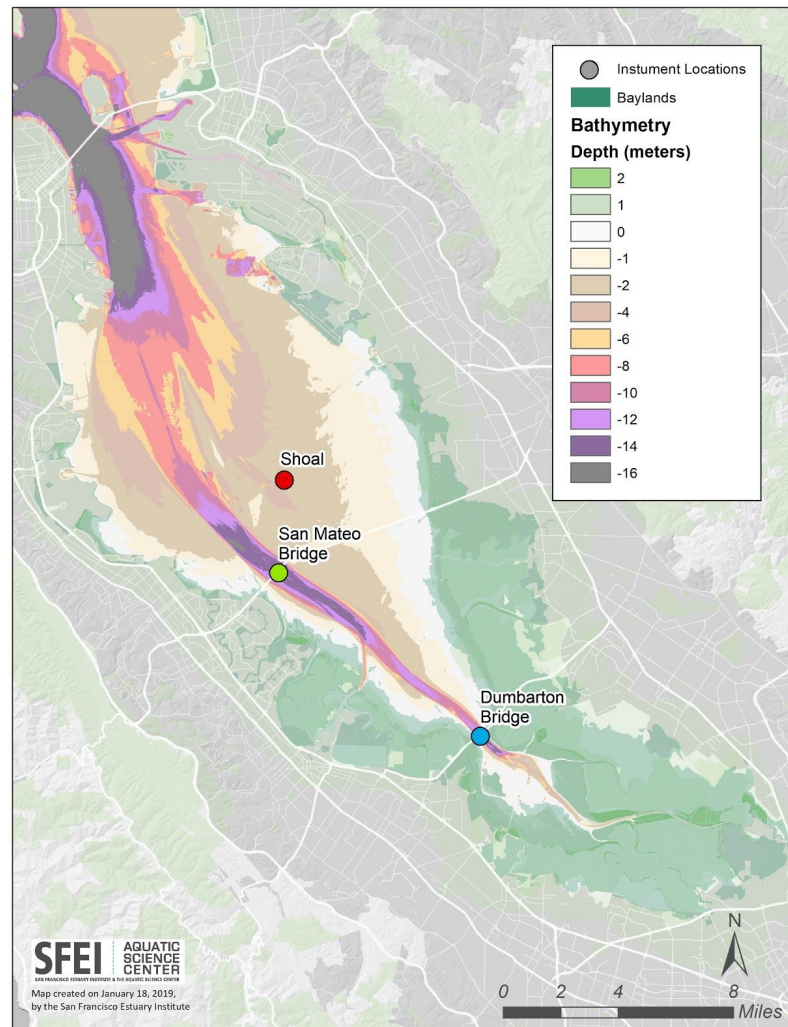

Figure 1. Bathymetry map of South Bay, including locations of mooring sites (Shoal, San Mateo Bridge, and Dumbarton Bridge).
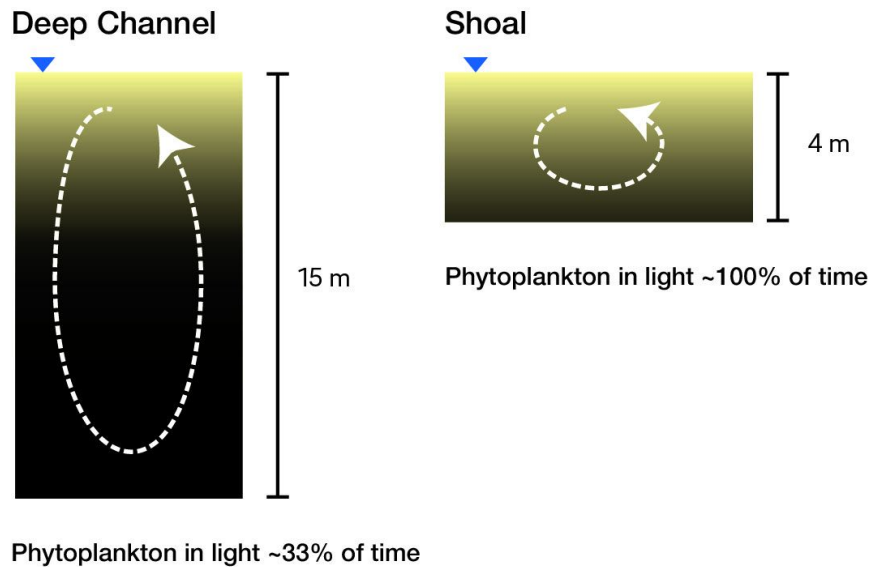
Figure 2: Schematic of South Bay the deep channel water column cross section (left) and the shoal water column cross section (right). Yellow to black indicate light levels as a function of depth, with light decreasing with depth, primarily due to suspended particulate matter (SPM). When both the channel and shoal regions are vertically well-mixed, phytoplankton experience very different light regimes. In this example, whereas in shoal regions phytoplankton can harvest light over the entire water column, in channel environments phytoplankton can only harvest light ⅓ of the time. As a result, average phytoplankton growth rates in shoal environments will substantially exceed those in channel environments. .

1.3 Goals of Study

The aim of these deployments was to quantitatively compare high frequency shoal conditions with observations in the deep channel. SFEI maintains a network of eight high frequency water quality sensors throughout the Lower South Bay, which we were able to use for direct comparisons with the shoal measurements. In this report, we focus on comparing the shoal data with our high frequency data at the San Mateo Bridge and Dumbarton Bridge. The specific goals were to:

1. Quantitatively characterize how shoal conditions are similar/different from channel observations.

2. Estimate and compare gross primary production (GPP) at shoal and channel sites during deployments.

3. Evaluate the need for a longer-term shoal mooring for further developing our understanding of water quality dynamics in the San Francisco Bay.

2. Methods

2.1 Instrument Deployment

SFEI, in partnership with the USGS California Water Science Center, deployed a mooring package in the shoal environment on three separate occasions:

- Spring 2017: March 20, 2017 — April 26, 2017
- Spring 2018: April 3, 2018 — May 23, 2018
- Fall 2018: September 5, 2018 — October 24, 2018

Figure 1 shows the location of the shoal mooring package relative to the moored sensor stations at the San Mateo and Dumbarton Bridges (N37.630789° W122.243200°). The shoal mooring instrument package was deployed approximately 4.5 kilometers north of the San Mateo Bridge (USGS Station 373751122143601). The instrument package was deployed on the bed, and ranged in depth between 2-5 meters depending on tidal stage. Each deployment consisted of two instrument packages (Figure 3), with one containing a stainless steel cage with water quality instruments, and the other containing an AquaDOPP water velocity instrument (Nortek, Boston, MA). Table 1 presents a list of instruments deployed.

Figure 3: Water-quality instruments mounted on stainless steel cage (left) and Aquadopp mounted on stainless-steel base plate (right).

Table 1: Water-quality instruments and additional equipment used during shoal mooring deployment

Instrument	Manufacturer	Parameters
DH4	Sea-Bird Scientific	NA (Data logger)
SUNA	Sea-Bird Scientific	Nitrate
ECO FLNTU	Sea-Bird Scientific	Chlorophyll-a
SBEE-CTD-37SI	Sea-Bird Scientific	Conductivity, Temperature, Depth
Pump	Sea-Bird Scientific	NA

EXO2	YSI	Temperature, Depth, Chlorophyll-a, Salinity, Dissolved Oxygen, Turbidity, Dissolved Organic Matter
AquaDopp	Nortek	Vertical profile of velocity
Pinger	RJE International	Package location

Most measurements were collected at 15-minute intervals using a mean calculated by 30-second burst sampling, except for the Aquadopp. Aquadopp measurements were made every minute and averaged across the 15-minute interval. Every 15 minutes, a pump with a 1 mm mesh screen was used to draw samples through the Sea-Bird CTD, SUNA, and ECO instruments connected with Tygon plasticizer-free tubing (Saint-Gobain Performance Plastics, Malvern, PA). The flow-through system was controlled using an in situ sensor interface module (DH4, Sea-Bird Scientific, Bellevue, WA). The EXO2 and Aquadopp were independently powered and logged data internally.

Instrument packages were serviced at approximately bi-weekly intervals. Upon retrieval, instruments were cleaned and data was downloaded. The EXO2 was swapped with a different EXO2 instrument each service and returned to the laboratory for a calibration check.

The data presented in this report are from the EXO2 instrument for all water quality parameters with the exception of salinity and nitrate. The EXO2 specific conductivity sensor experienced fouling with each deployment, thus we used the salinity data form the SBEE-CTD-37SI. Nitrate was only collected with the SUNA instrument. We focused the shoal analysis on the EXO2 data because the instruments at San Mateo and Dumbarton Bridge are also EXO2s.

2.2 Discrete sample methods

Water-quality samples were collected for chlorophyll-a, pheophytin-a, phycocyanin, nutrients (total nitrogen, ammonia, nitrate, nitrite, and orthophosphate), and suspended sediment concentration (SSC) over each deployment period during trips to service instruments. Typically, a sample was collected upon arrival to the station, before instruments were serviced, and a second time before departure. Water was collected by deploying a van Dorn sampler (non-isokinetic sampler) to a depth slightly above the instrument package. Pigment and SSC samples were split into amber 1L HDPE wide-mouth bottles and pre-tared opaque 1L HDPE wide-mouth bottles, respectively (Nalgene, Rochester, NY). Nutrients were collected into a 500 mL HDPE bottle and immediately filtered through an in-line 0.45 capsule filter (Pall, Port Washington, NY) into a 125 mL amber HDPE bottle. All water samples were immediately placed in a dark cooler on ice. Chlorophyll-a samples were filtered within 24 hours of collection using a GF/F filter (Advantec, Dublin, CA) and light suction (<10 psi).

Chlorophyll-a and nutrient samples were analyzed by the USGS National Water Quality Lab in Denver, CO. Chl-a was determined using EPA method 445.0 (Arar and Collins, 1997). Nitrate plus nitrite was determined colorimetrically after enzymatic reduction, following the method of Patton and Kryskalla (2011). Total dissolved phosphorus and nitrogen was analyzed following a persulfate digestion using the method of Patton and Kryskalla (2003).

2.3 Primary Productivity Modeling

To estimate gross primary productivity (GPP) we use the following equation from Jassby et al. (2002):

$$GPP = \frac{4.6 * \Psi * B * I_o}{kd}$$

where Ψ is the light utilization efficiency (0.82 mg C/mg Chl-a) for the San Francisco Bay, B is the chlorophyll-a measurement (mg/m^3), I_o is photosynthetically active radiation (PAR; units of E/m^2 d, where E, einstein = 1 mol of photons), and kd is the light extinction coefficient (1/m). The derived equation from Jassby et al. (2002) assumes "PAR does not change with depth, water column depth exceeds photic zone depth, Chl a is vertically homogeneous, and primary productivity is proportional to light absorbed by photosynthetic pigments."

In order to calculate net primary productivity (NPP), we calculate the difference between GPP and respiration of phytoplankton (R):

$$NPP = GPP - R$$

Where R is calculated as described in Jassby et al. (2002):

$$R = 0.015 * w * B * H + 0.015 * GPP$$

With w representing the carbon to chlorophyll-a ratio of 35 (Cloern et al. 1995), and H is water column depth (m).

For incident light, we used solar radiation data from the Union City meteorological station (N37.598758 W122.05323), which is part of the California Irrigation Management Information System (CIMIS) station network. The solar radiation data is collected in W/m^2. In order to convert from W/m^2 to PAR, we used the conversion established by Morel and Smith (1974):

$$PAR = Solar\ radiation * \frac{86,400\ seconds\ day^{-1} * 2.77e18\ quanta\ s^{-1} W^{-1}}{6.02e23\ quanta\ Einstein^{-1}}$$

To calculate the light extinction coefficient (kd), we used a linear regression equation (Figure 4) developed between high frequency turbidity data measurements using an EXO2 at the Dumbarton Bridge and measured light extinction coefficient measurements (kd) at station 33 of the USGS R/V Peterson cruise (station 33 is closest to Dumbarton Bridge).
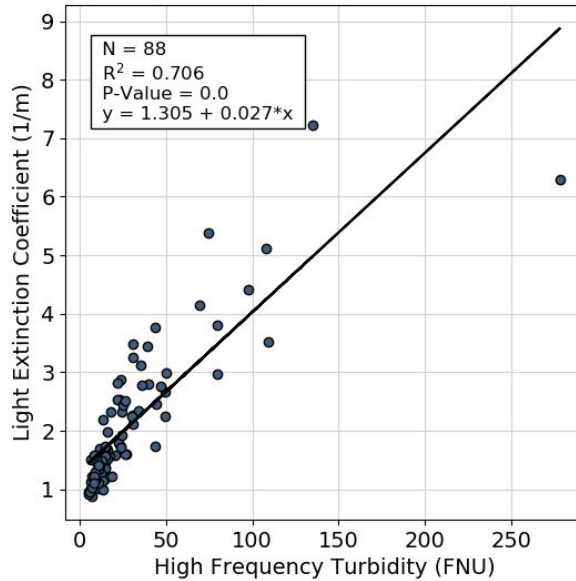
Figure 4: High frequency turbidity vs. light extinction coefficient measurements at station 33 of the USGS R/V Peterson cruise. Turbidity is shown in formazin turbidity units (FNU).

Therefore, in order to estimate light extinction coefficient from the high frequency turbidity data, we used the following equation:

$$kd = 1.305 + 0.027 * Turbidity$$

3. Results and Discussion

Tables 2 and 3 present the mean and standard deviation of the hourly averaged data for each site over the three deployment periods. For spring 2017, the mean and standard deviation for the San Mateo Bridge site are not presented in the tables because the site experienced extreme fouling midway through the deployment, and thus a significant portion of the data was removed (seen in Figure 5). The time periods used for each deployment calculation were (they vary slightly from the time periods listed above due to instruments failing at the end of the Spring 2017 and Spring 2018 deployments):

– Spring 2017: March 20, 2017 to April 22, 2017
– Spring 2018: April 3rd, 2018 to May 19th, 2018
  ○ For salinity and depth we used the time period of April 13th, 2018 to May 19th, 2018. This was because the CTD failed upon initially being deployed, but was restored on April 13th.
– Fall 2018: Sept 5th, 2018 to October 24th, 2018

Sections 3.1, 3.2, and 3.3 provide a detailed discussion of the differences between parameters for each deployment. In these sections, Figures 5, 6, and 7 present the results from the spring 2017, spring 2018,

and fall 2018 deployments, respectively. Discrete chlorophyll concentrations were consistent with high frequency in situ measurements (Figure A.1), therefore, only high frequency data are presented here.

Table 2: Mean ± standard deviation of each parameter for each site for the three deployment periods.

	Spring 2017			Spring 2018			Fall 2018		
	Shoal	**DMB**	**SMB**	**Shoal**	**DMB**	**SMB**	**Shoal**	**DMB**	**SMB**
Chlorophyll (µg/L)	19.62 ±13.83	6.80 ±3.36	—	6.25 ±3.90	12.77 ±6.08	2.79 ±0.99	5.76 ±1.80	3.33 ±0.96	1.92 ±0.65
Turbidity (FNU)	17.55 ±19.11	38.36 ±42.7	—	9.02 ±6.52	44.98 ±46.84	8.62 ±8.23	18.60 ±13.36	27.25 ±18.83	20.59 ±18.35
Nitrate (µM)	17.54 ±6.89	—	—	—	—	—	31.68 ±5.26	—	—
DO (mg/L)	9.67 ±1.16	8.34 ±0.37	—	8.82 ±1.16	8.15 ±1.43	8.09 ±1.27	7.29 ±0.27	7.02 ±0.46	6.36 ±0.22
Salinity (PSU)	16.96 ±1.21	14.43 ±1.67	—	23.81 ±0.59	22.91 ±0.82	23.59 ±0.64	31.29 ±0.17	30.71 ±0.68	31.03 ±0.11
Temperature (°C)	15.35 ±0.61	15.66 ±0.83	—	16.88 ±0.92	17.74 ±1.08	17.07 ±0.75	19.36 ±0.62	20.01 ±0.81	19.58 ±0.64
Depth (m)	3.97 ±0.61	2.85 ±0.69	—	3.68 ±0.69	2.86 ±0.77	3.71 ±0.75	3.96 ±0.51	2.91 ±0.73	4.14 ±0.67

3.1 Spring 2017

During the Spring 2017 deployment, the chlorophyll at the shoal was notably higher than at DMB and SMB for the first half of the deployment (Figure 5). Around April 7th/8th, the chlorophyll magnitude at the shoal dampened. This dampening coincided with a sustained increase in turbidity at the shoal and DMB (SMB experienced bio-fouling during this time, and thus the data are not presented). Throughout the deployment, the turbidity of DMB and the shoal showed similar patterns, however, DMB was consistently higher than the shoal. Nitrate measured at the shoal (nitrate is not measured at DMB and SMB) closely tracked chlorophyll throughout the deployment. The nitrate concentrations began in the range of 20-30 µM, and then decreased as the chlorophyll magnitude increased (indicating nitrate consumption by phytoplankton). Following this decrease, the chlorophyll and nitrate oscillated together for a couple weeks, and then nitrate returned to a magnitude close to 20 µM during the period when chlorophyll was low and turbidity high. As chlorophyll started to increase again toward the end of the deployment, nitrate once again began to decrease. The three sites had very similar measurements of DO, salinity, and temperature, with the shoal having slightly higher sustained magnitudes of DO and salinity.
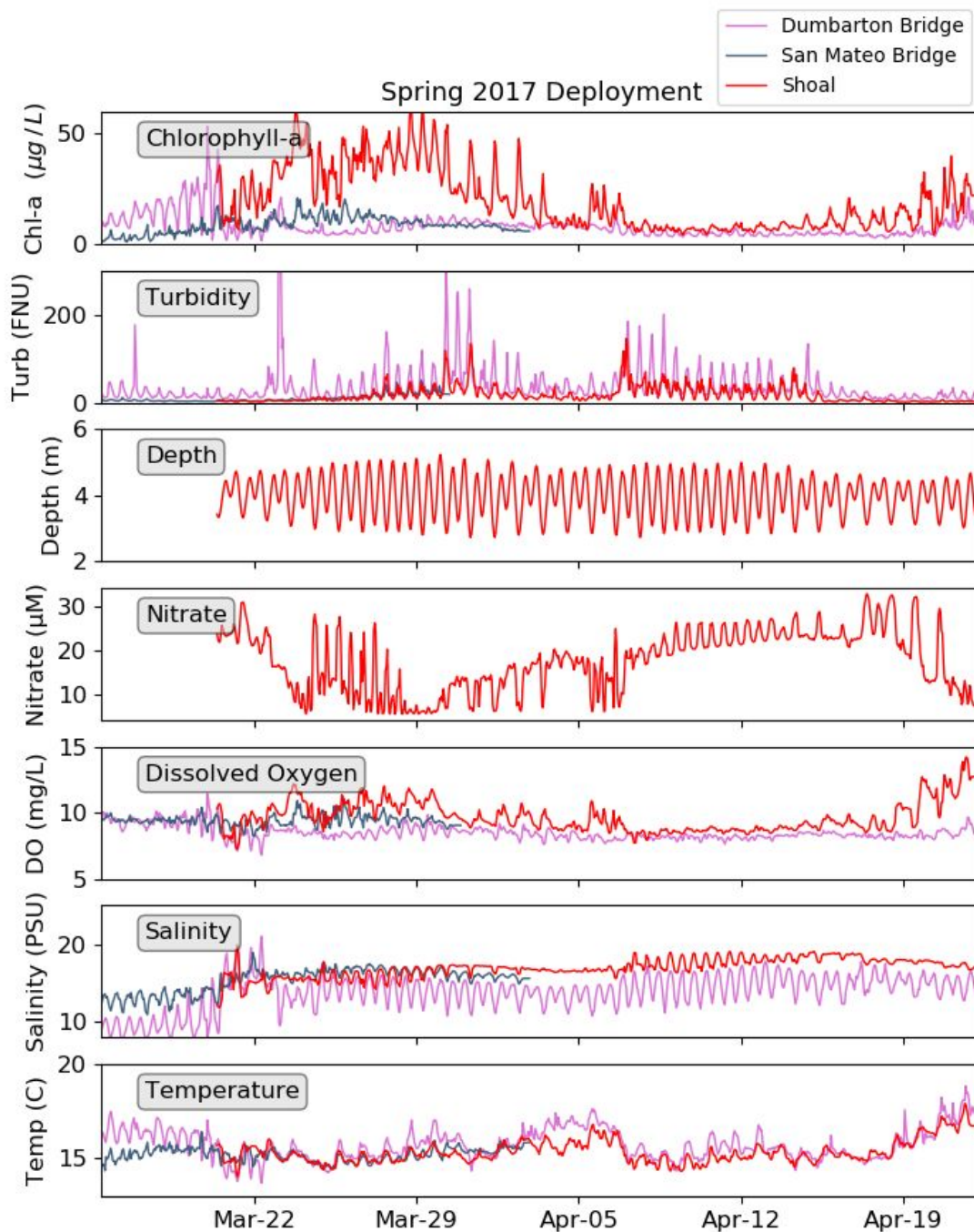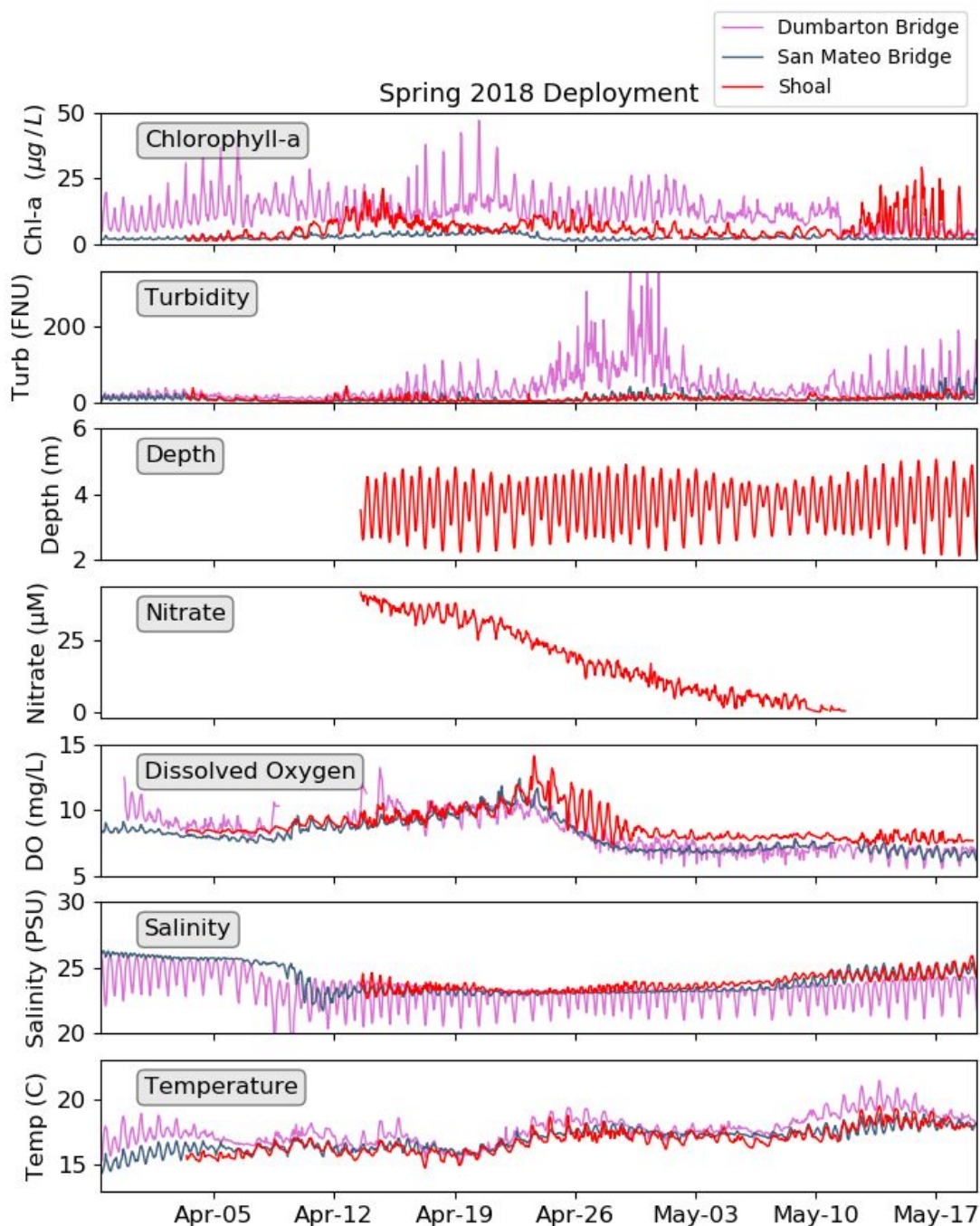
Figure 5: Results from the spring 2017 deployment for the shoal, Dumbarton Bridge, and San Mateo Bridge high frequency monitoring sites.

3.2 Spring 2018

In the Spring, 2018 deployment, the chlorophyll magnitude was greater at DMB compared with the shoal for the majority of the deployment (Figure 6). Only in the final week of the deployment did the chlorophyll magnitude at the shoal exceed that at DMB. Chlorophyll at SMB remained relatively low for the entire deployment and was consistently less than DMB and the shoal. Turbidity levels were similar at

all three sites at the beginning of the deployment, however, starting around mid-April there was a sustained uptick in turbidity at DMB but not at SMB or the shoal. Although plotted, the nitrate data were invalid for this time period (due to a problem with the lamp on the SUNA nitrate sensor). DO was similar at the three sites, although the shoal sustained slightly greater DO values starting around April 23rd. DMB showed the greatest variance in salinity, with the shoal more closely resembling the muted salinity signal at SMB. Temperature was very similar at the three sites.

Figure 6: Results from the spring, 2018 deployment for the shoal, Dumbarton Bridge, and San Mateo Bridge high frequency monitoring sites.

3.3 Fall 2018

In the fall, 2018 deployment, the chlorophyll magnitude at the shoal was consistently greater than at DMB and SMB (Figure 7). Additionally, chlorophyll showed a stronger tidal signal at the shoal compared with DMB and SMB. Turbidity magnitudes were similar at the three sites, although there were occasional turbidity spikes at DMB and SMB that were not seen in the shoal. Nitrate generally remained above 20 µM, and demonstrated tidal fluctuations throughout the deployment. DO showed the most variability at DMB, and generally had the greatest magnitude at the shoal. Salinity also showed the most variability at DMB, with muted tidal signals at SMB and the shoal. Temperature was very similar for the three sites.
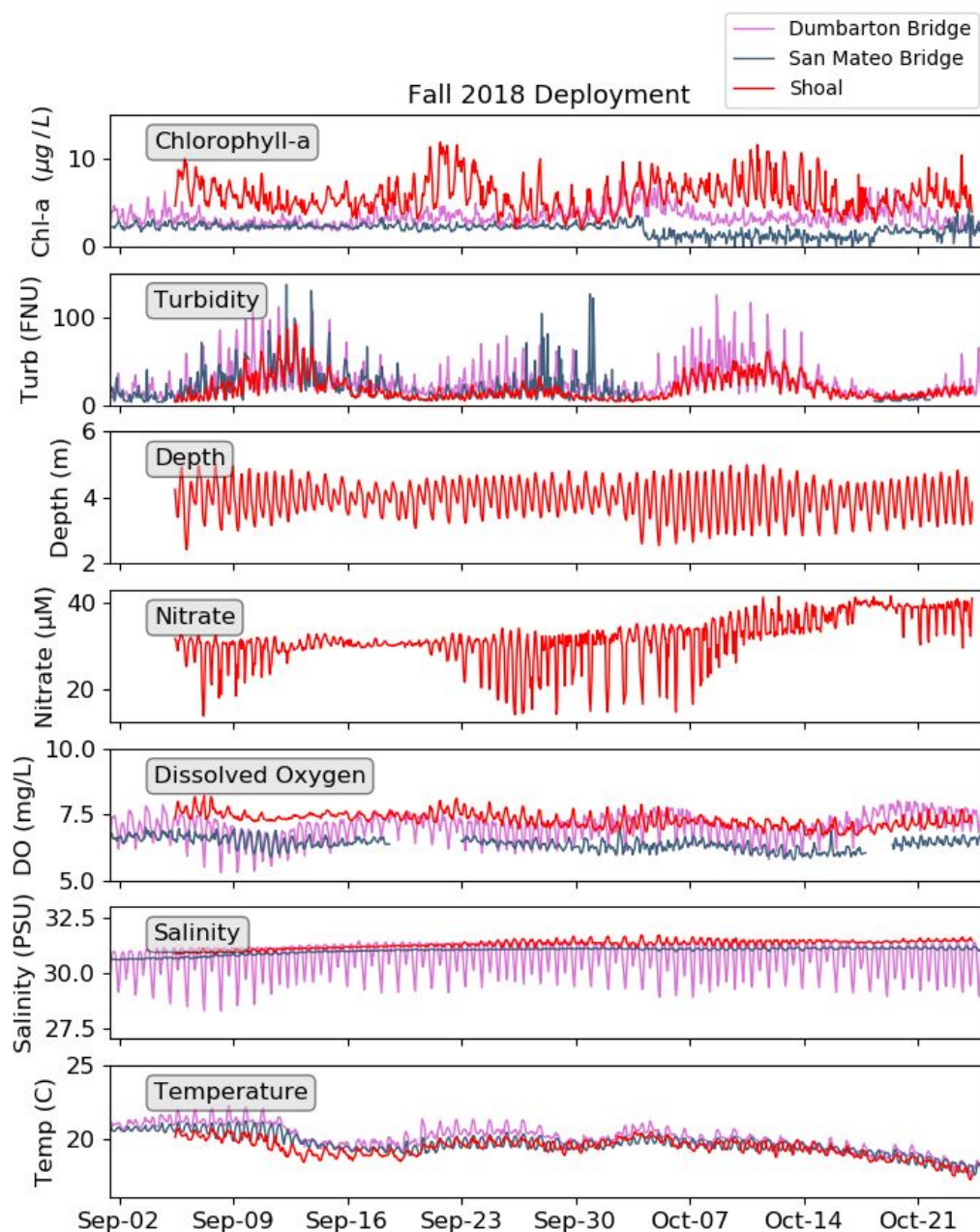

Figure 7: Results from the fall, 2018 deployment for the shoal, Dumbarton Bridge, and San Mateo Bridge high frequency monitoring sites.

3.4 Nitrate and Chlorophyll

Figure 8 displays a time series of nitrate and chlorophyll data at the shoal station for spring 2017. These two time series track each other, with nitrate generally low when chlorophyll is high, and vice versa. At the beginning of the time series, nitrate decreased as chlorophyll gradually increased. When chlorophyll was sustained near its maximum magnitude for several days, nitrate dropped down close to 5 µM (near the detection limit of the SUNA instrument). Around March 30th, nitrate concentrations began to rise, then quickly decreased when there was a spike in chlorophyll, which subsequently happened two more times. During the period when chlorophyll remained low (during the sustained turbidity uptick discussed in Section 3.1), nitrate levels increased and remained high (between 20-25 µM). At the end of the deployment, chlorophyll concentrations began to increase once again, with a corresponding decrease in nitrate concentrations. Figure 9 displays a scatterplot of the same spring 2017 data, with nitrate concentrations represented by the color of the scatter points. This figure illustrates that DO generally increased with chlorophyll concentrations during the spring deployment. It also shows that high nitrate concentrations corresponded with low chlorophyll, and vice versa.
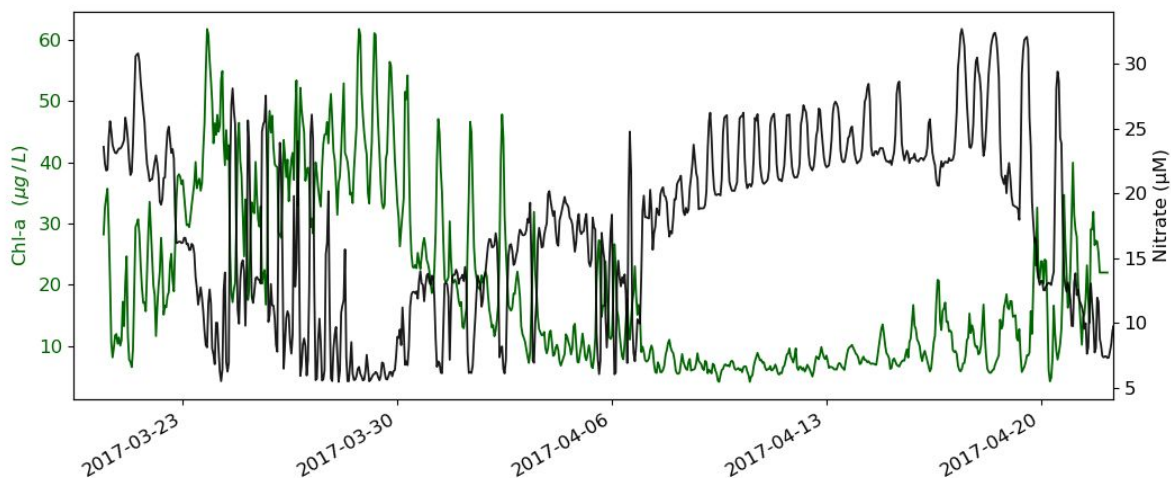

Figure 8: Time series of chlorophyll-a (green) and nitrate (black) at the shoal site for spring, 2017.
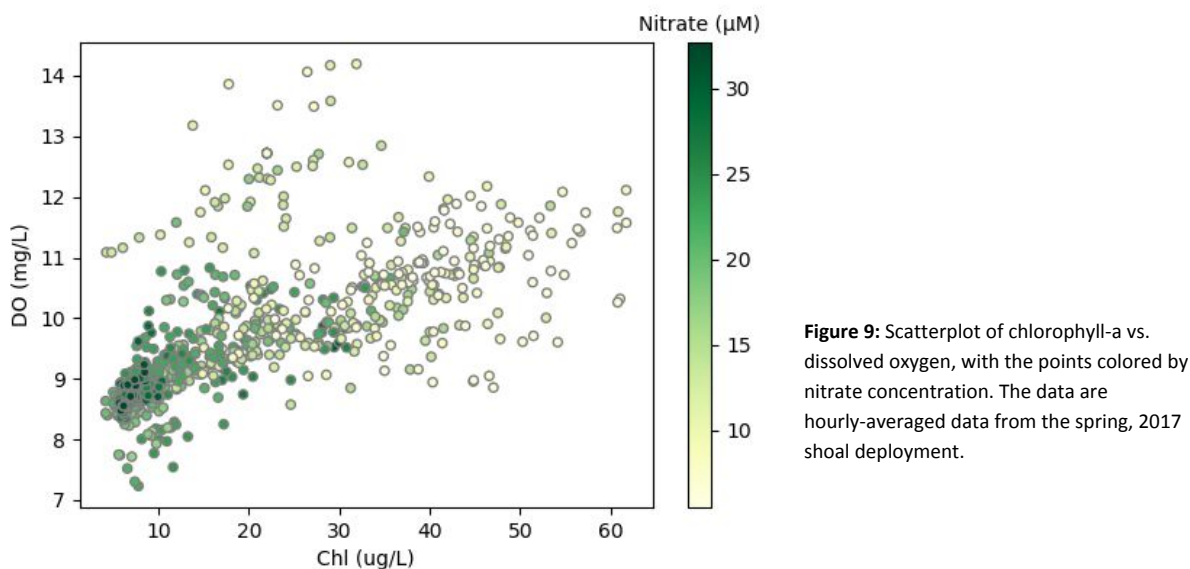

Figure 9: Scatterplot of chlorophyll-a vs. dissolved oxygen, with the points colored by nitrate concentration. The data are hourly-averaged data from the spring, 2017 shoal deployment.

Nitrate data for spring 2018 were discarded due to data quality issues, and thus are not presented here. Figure 10 presents the chlorophyll/nitrate data for the fall 2018 deployment. Compared with the spring 2017 time series, the chlorophyll in fall 2018 was lower and the nitrate was higher. The nitrate did not trend down toward 5 µM as was the case in the spring 2017 data; nitrate remained at high magnitudes throughout the entire fall 2017 time series. There were some quick drops in nitrate concentrations that generally aligned with spikes in chlorophyll, but these decreases in nitrate were brief. Similar to the spring 2017 deployment, there was a general trend for DO to increase with high levels of chlorophyll (Figure 11). The pattern between chlorophyll and nitrate, however, was not as clear. Although higher levels of nitrate tended to correspond to low concentrations of chlorophyll, this trend was not consistent throughout the timeseries.
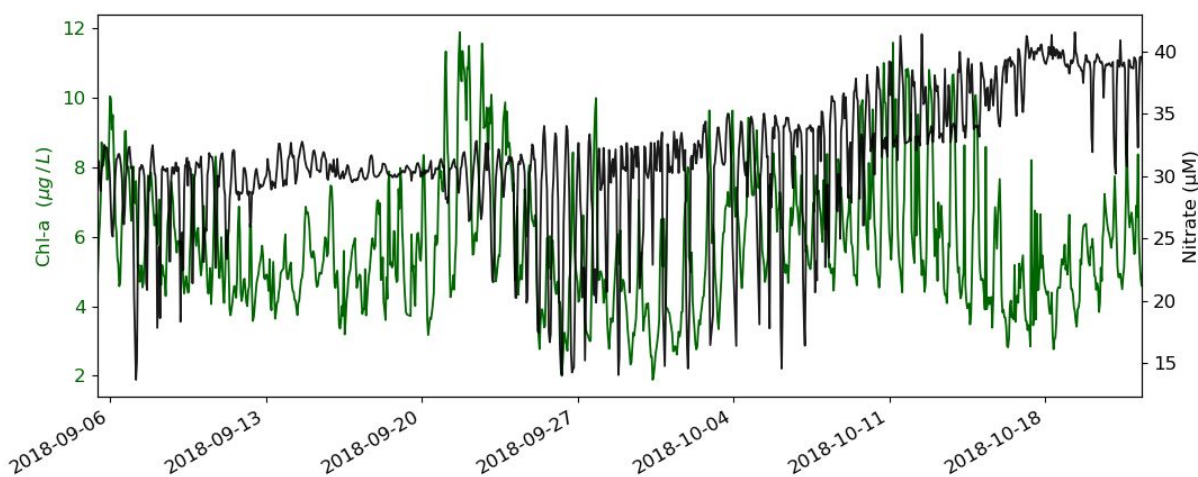

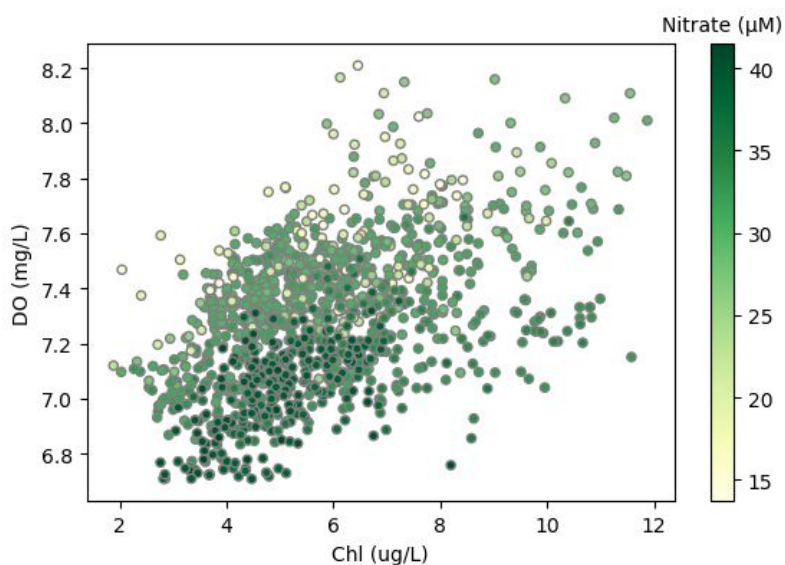**Figure 10:** Time series of chlorophyll-a (green) and nitrate (black) at the shoal site for fall 2018.

Figure 11: Scatterplot of chlorophyll-a vs. dissolved oxygen, with the points colored by nitrate concentration. The data is hourly-averaged data from the fall 2018 shoal deployment.

3.5 Gross Primary Production (GPP)

For each of the three stations, we calculated an envelope (min and max) of daily GPP values based on hourly measurements from each day. Therefore, for each site and each day we calculated 24 daily GPP values by interpolating hourly GPP values to daily values. This is based off the assumption that the measurements made by the instrument are a temporal/spatial snapshot of water, and each parcel of water that passes by the instrument continues to fix carbon throughout the rest of the day. Therefore, we assume that each measurement parcel continues production at the same rate throughout the entire day. In making these daily GPP calculations for each one-hour measurement, we use a 24-hour rolling average of weather conditions surrounding the measurement hour (therefore we capture both day and night conditions). Also in this calculation we use the hourly chlorophyll and light extinction coefficient data, which assumes that the parcel maintains constant levels of chlorophyll and turbidity throughout the day. Calculating daily GPP estimates for each hourly measurement gives 24 daily GPP estimates in the zone of influence of each site.

Figure 12 displays a time-series envelope of the maximum and minimum GPP estimates for each day (of the 24 daily GPP estimates for each day, the top line of the envelope represents each maximum daily estimate, and the bottom line represents each minimum daily estimate). In spring 2017, the rates of GPP were consistently higher on the shoal than in the channel for the duration of the season, with some large peaks between March 21 and April 4, and again at the end of the deployment after April 18. In spring 2018, both the shoal and Dumbarton Bridge stations had high but variable GPP values, with several peaks occurring throughout the deployment period of up to 6 gC m^{-2} day^{-1}. GPP in fall 2018 was low for all stations, with values at Dumbarton and San Mateo consistently around 1 gC m^{-2} day^{-1}. Values at the shoal station were only slightly higher, reaching peaks at around 3 gC m^{-2} day^{-1}.
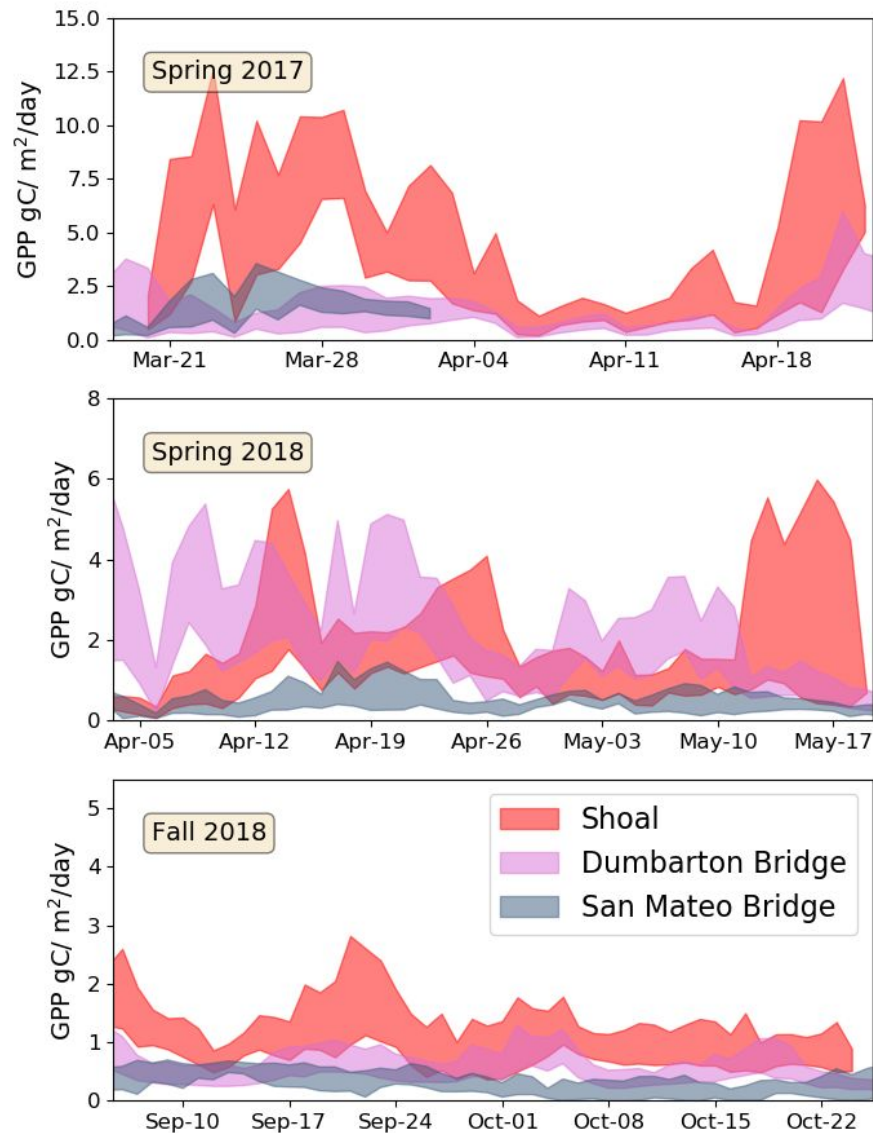
Figure 12: Daily GPP estimates at each of the three high frequency sites. The envelope plotted for the high frequency sites represents the range of the maximum and minimum estimates for each 24-hour period. The top panel is the spring 2017 deployment, the middle panel is the spring 2018 deployment, and the bottom panel is the fall 2018 deployment.

4. Conclusions and Next Steps

The deployments of the shoal mooring demonstrated that simultaneous high frequency measurements of multiple parameters can help elucidate drivers of water quality patterns. The data collected from the shoal station indicate that turbidity, which limits light availability, can exert strong control over chlorophyll concentrations. For example, a turbidity spike on the shoal in spring 2017 coincided with a rapid decrease in chlorophyll. Despite occasional increases, turbidity tended to be lower on the shoal compared to the San Mateo and Dumbarton stations, which is consistent with patterns in chlorophyll that were observed. Chlorophyll and GPP tended to be higher on the shoal

compared to the channel stations, indicating that this area of the bay may support high levels of productivity. There were interesting patterns between the chlorophyll and nitrate data, with an inverse relationship between the two parameters. Increases in chlorophyll coincided with a clear drawdown of nitrate. This inverse relationship suggests phytoplankton could be experiencing nitrate limitation on the shoals.

Overall, comparisons of chl-a and calculated GPP between shoal and channel environments suggest that sustained shoal observations are needed to capture the distinct conditions there. While the large differences in 'biogeochemical condition' between these adjacent habitats are themselves intriguing in terms of their underlying root physical and ecological causes, the fact that shallow/shoal habitats comprise the majority of area of several SFB subembayments (South Bay, Lower South Bay, San Pablo Bay, Suisun Bay) argues that those biogeochemical differences (weighted by area) could also be meaningful from management and regulatory perspectives (e.g. do we reach a different conclusion about trophic status when area-weighted GPP is used?). The possibility of sustained nitrate-limiting growth conditions for phytoplankton also deserves further investigation. If, on the one hand, nitrate (or, more generally, DIN) concentrations, do not substantially influence phytoplankton growth rates, then increasing (or decreasing) N loads to the system may not appreciably influence phytoplankton production. If, on the other hand, growth-limiting nitrate concentrations occurs more widely (or for longer duration) in SFB, then changing nutrient inputs from wastewater dischargers could influence phytoplankton production. Finally, given the early-stage analysis of these data, it is important to (re)emphasize that making interpretations about the ecological or regulatory/management significance of these differences would be premature. However, observations and analysis to date clearly indicate that further investigation is warranted.

5. References

Arar, E. J. and G. B. Collins. Method 445.0 In Vitro Determination of Chlorophyll a and Pheophytin ain Marine and Freshwater Algae by Fluorescence. U.S. Environmental Protection Agency, Washington, DC, 1997.

Cloern, J. E., C. Grenz, and L. Vidergar-Lucas. 1995. An empirical model of the phytoplankton chlorophyll:carbon ratio - The conversion factor between productivity and growth rate. Limnology and Oceanography 40: 1313-1321.

Jassby, A. D., J. E. Cloern, and B. E. Cole. 2002. Annual primary production: patterns and mechanisms of change in a nutrient-rich tidal ecosystem. Limnology and Oceanography 47: 698-712.

Morel, A. and R.C. Smith. 1974. Relation between total quanta and total energy for aquatic photosynthesis. Limnology and Oceanography 19: 591-600.

Patton, C.J. and J.R. Kryskalla. 2003. Methods of analysis by the US Geological Survey National Water Quality Laboratory: evaluation of alkaline persulfate digestion as an alternative to Kjeldahl digestion for determination of total and dissolved nitrogen and phosphorus in water No. 2003-4174. U.S. Geological Survey Techniques and Methods.

Patton, C.J. and J.R. Kryskalla. 2011. Colorimetric determination of nitrate plus nitrite in water by enzymatic reduction, automated discrete analyzer methods. US Geological Survey Techniques and Methods.

Thompson, J.K., J.R. Koseff, S.G. Monismith, and L.V. Lucas. 2008. Shallow water processes govern system-wide phytoplankton bloom dynamics: A field study. Journal of Marine Systems 74: 153-166.
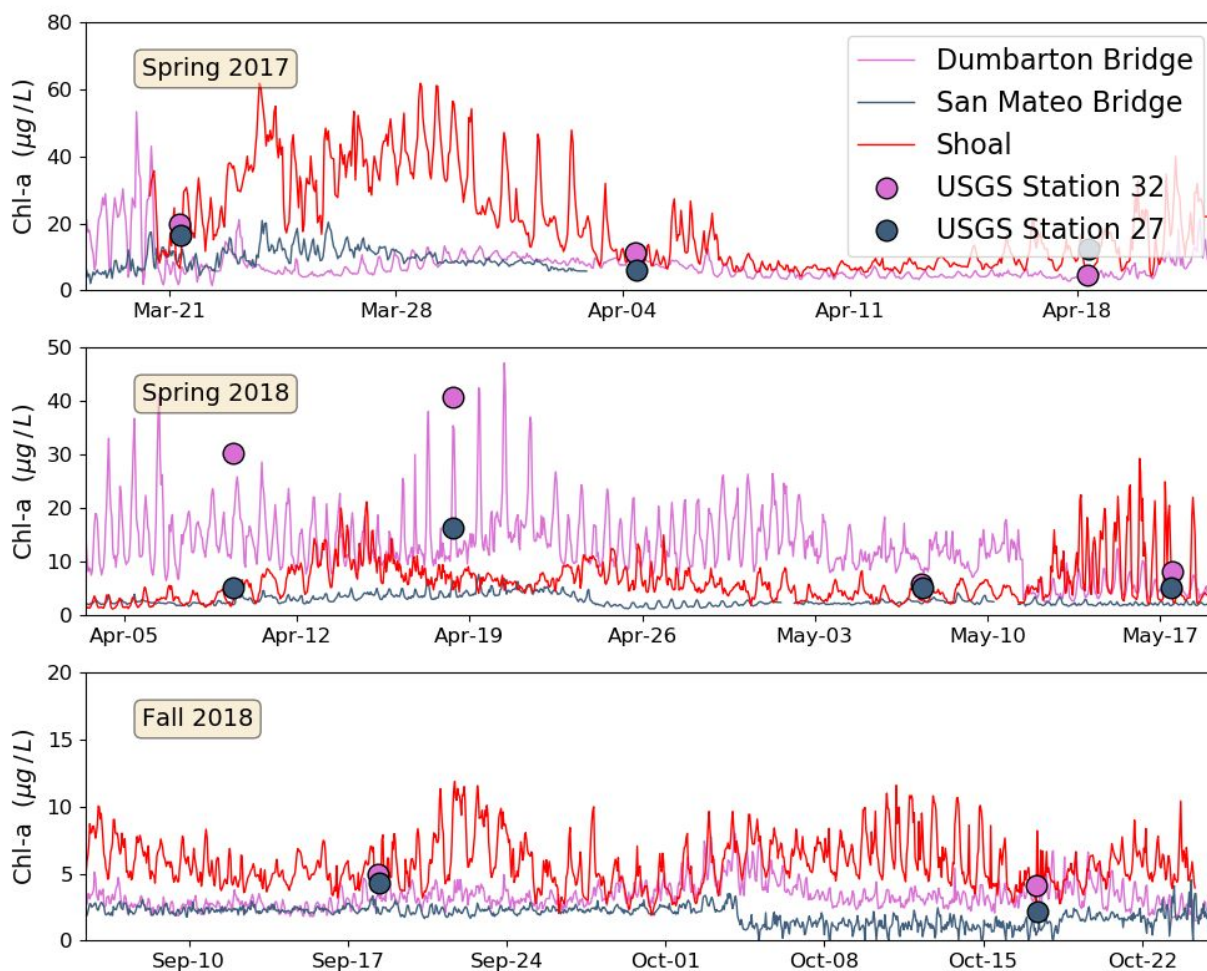
6. Appendix

Figure A.1 Chlorophyll-a at high frequency mooring sites (Dumbarton Bridge, San Mateo Bridge and the Shoal station) and discrete chlorophyll measurements at USGS Station 32 (near Dumbarton Bridge) and Station 27 (near San Mateo Bridge) for each shoal deployment period.